

First-principles study on the intermediate compounds of LiBH_4

Nobuko Ohba, Kazutoshi Miwa, Masakazu Aoki, Tatsuo Noritake, and Shin-ichi Towata
Toyota Central Research & Development Laboratories, Inc., Nagakute, Aichi 480-1192, Japan

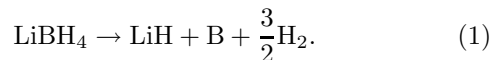
Yuko Nakamori, and Shin-ichi Orimo
Institute for Materials Research, Tohoku University, Sendai 980-8577, Japan

Andreas Züttel
Physics Department, University of Fribourg, Perolles, CH-1700 Fribourg, Switzerland
(Dated: November 2, 2013)

We report the results of the first-principles calculation on the intermediate compounds of LiBH_4 . The stability of LiB_3H_8 and $\text{Li}_2\text{B}_n\text{H}_n$ ($n = 5-12$) has been examined with the ultrasoft pseudopotential method based on the density functional theory. Theoretical prediction has suggested that monoclinic $\text{Li}_2\text{B}_{12}\text{H}_{12}$ is the most stable among the candidate materials. We propose the following hydriding/dehydriding process of LiBH_4 via this intermediate compound : $\text{LiBH}_4 \leftrightarrow \frac{1}{12}\text{Li}_2\text{B}_{12}\text{H}_{12} + \frac{5}{6}\text{LiH} + \frac{3}{12}\text{H}_2 \leftrightarrow \text{LiH} + \text{B} + \frac{3}{2}\text{H}_2$. The hydrogen content and enthalpy of the first reaction are estimated to be 10 mass% and 56 kJ/mol H_2 , respectively, and those of the second reaction are 4 mass% and 125 kJ/mol H_2 . They are in good agreement with experimental results of the thermal desorption spectra of LiBH_4 . Our calculation has predicted that the bending modes for the Γ -phonon frequencies of monoclinic $\text{Li}_2\text{B}_{12}\text{H}_{12}$ are lower than that of LiBH_4 , while stretching modes are higher. These results are very useful for the experimental search and identification of possible intermediate compounds.

I. INTRODUCTION

Hydrogen is the most promising environmentally clean energy carrier to replace fossil fuels. The use of hydrogen-based energy in practical applications such as fuel cell vehicles, however, requires the development of safe and efficient hydrogen storage technology. Complex hydrides including the light metal lithium (Li) have sufficient gravimetric hydrogen storage capacity, and many researches and development about the lithium complex hydride such as LiBH_4 ^{1,2,3} and LiNH_2 ^{4,5,6} have been done recently. Particularly, LiBH_4 can desorb about 14 mass% of hydrogen by the following thermal decomposition :



However, the experimental value of enthalpy of this reaction is 69 kJ/mol H_2 ¹ and LiBH_4 is too stable to release hydrogen at ambient condition. High temperature and high pressure are needed for rehydriding reaction, so its reversibility becomes a problem for practical use.

Züttel *et al.*¹ investigated the hydrogen desorption from LiBH_4 in details, and reported that the thermal desorption spectra of LiBH_4 mixed with SiO_2 -powder exhibited three hydrogen desorption peaks. These peaks were observed around 500 K, 550 K and 600 K, and the products corresponded to “ $\text{LiBH}_{3.6}$ ”, “ LiBH_3 ” and “ LiBH_2 ”, respectively. The compounds in quotes were nominal compositions estimated from amount of desorbed hydrogen. This is a strong evidence for the existence of the intermediate compounds, and the hydrogen desorption reaction takes place in at least two steps not a single step like in Eq.(1). Although low temperature release of hydrogen and improvement of reversibility can be expected

by use of the intermediate compound, little attention has been paid yet.

In this study, the stability of the intermediate compounds of LiBH_4 has been investigated theoretically and we clarify a hydriding/dehydriding process of LiBH_4 . The thermal desorption experiment observed a structural transition around 380 K and the melting of the compound at 550 K. The stability of the solid phases at absolute zero temperature is mainly discussed here. In Sec. II, we describe the details of the computational method and the possible intermediate compounds of LiBH_4 . Section III reports the calculated results on the stability of some candidate compounds. And then, we discuss the hydriding/dehydriding reaction via the intermediate compounds. Furthermore, the electronic structures and Γ -phonon frequencies on the most stable compound are studied. We also investigate the stability of the borane complex anions, and then compare with the solid compounds.

II. COMPUTATIONAL DETAILS

First-principles calculations have been performed by the ultrasoft pseudopotential method⁷ based on the density functional theory.⁸ The generalized gradient approximation (GGA) formula⁹ is applied to the exchange-correlation energy.

The interaction between the ion cores and electrons is described by the ultrasoft pseudopotential⁷, and the norm-conservation constraint¹⁰ is imposed on Li for the calculation efficiency improvement. The scalar-relativistic all-electron calculations are first carried out on the free atoms(ions). We chose $2s$ and $2p$ states for

both Li and B pseudopotential as the reference states with the cutoff radii of 2 a.u. (Li) and 1.5 a.u. (B), respectively. A single projector function is used for each angular momentum component. The $3d$ state is treated as the local part of pseudopotential. The hydrogen pseudopotential is constructed from $1s, 2s$ and $2p$ states with the cutoff radii of 1.1 a.u. (s) and 1.2 a.u. (p). We use double projector functions for the s component and a single projector function for the p component. For all pseudopotentials, the pseudo-wave functions and the pseudo-charge-augmentation functions are optimized by a method similar to that proposed by Rappe *et al.*¹¹ Also, the partial core correction¹² is taken into account for Li and B pseudopotentials.

In the solid-state calculations, the pseudo-wave functions are expanded by plane waves with a cutoff energy equal to 15 hartrees. The cutoff energy for the charge density and potential is set to be 120 hartrees. The integral over the Brillouin zone is approximated by the summation on the \mathbf{k} -grid elements of which the edge lengths closer to the target value of 0.15\AA^{-1} as possible. We confirmed that these calculation conditions gave a good convergence of energy within 0.002 eV/atom. The preconditioned conjugate-gradient technique is employed to minimize the Kohn-Sham energy functional. A procedure based on the iterative diagonalization scheme¹³ and the Broyden charge mixing method¹⁴ is adopted in this study. Optimization of crystal structures is performed till the atomic forces and the macroscopic stresses become less than 5×10^{-4} hartree/bohr and 0.1 GPa, respectively. During the structural optimization process, the partial occupation numbers near the Fermi level are determined by the Fermi-Dirac distribution function with $k_B T = 3 \times 10^{-3}$ hartrees. The Helmholtz free-energy functional,¹⁵ including the entropy term, is minimized instead of the Kohn-Sham energy functional. Then, the improved tetrahedron method¹⁶ is used in order to minimize the Kohn-Sham energy functional in the optimized structure. The dynamical matrix is calculated by the force-constant method¹⁷ to obtain the Γ phonon frequencies. The atomic displacement is set to be 0.02 \AA . The further details of calculation are described in Refs. 2, 13 and references therein.

As the candidates of the intermediate compounds, the existing alkali metal-B-H materials are used. For example, it is well known that boron (B) and hydrogen (H) form inorganic compounds called 'borane' and the compounds of CsB_3H_8 ,¹⁸ $\text{K}_2\text{B}_6\text{H}_6$,¹⁹ and $\text{K}_2\text{B}_{12}\text{H}_{12}$ ²⁰ are reported. The space group of crystal structure for the compound CsB_3H_8 is $Ama2$ (No.40) and cation Cs^+ and anion $[\text{B}_3\text{H}_8]^-$ are arranged same as the NaCl-type structure with an orthorhombic distortion. The crystal structures of $\text{K}_2\text{B}_6\text{H}_6$ and $\text{K}_2\text{B}_{12}\text{H}_{12}$ are best described as an anti- CaF_2 -type arrangement with K^+ cation in the center of a tetrahedron formed by $[\text{B}_n\text{H}_n]^{2-}$ dianions. We first assumed that LiB_3H_8 , $\text{Li}_2\text{B}_6\text{H}_6$ and $\text{Li}_2\text{B}_{12}\text{H}_{12}$ compounds, which had the same crystal structures as existing CsB_3H_8 , $\text{K}_2\text{B}_6\text{H}_6$ and $\text{K}_2\text{B}_{12}\text{H}_{12}$, respectively. The

stability of these candidates was evaluated using the first-principles calculations. Since the existence of a series of *closo*-type dianions $[\text{B}_n\text{H}_n]^{2-}$ ($n = 5 - 12$) is also well known, our calculation have been expanded to $\text{Li}_2\text{B}_n\text{H}_n$ ($n = 5 - 12$) compounds. Although Li atom and $[\text{B}_n\text{H}_n]$ cluster are arranged in the anti- CaF_2 -type structure and the unit cell parameters are supposed to be a face-centered-cubic symmetry ($a = b = c, \alpha = \beta = \delta = 90^\circ$) as starting points for the structural optimization, the output relaxed compounds have different symmetry depending on the structure of $[\text{B}_n\text{H}_n]$ clusters. The alkali metal salt of monoclinic $\text{K}_2\text{B}_{12}(\text{OH})_{12}$ ²¹ with *closo*- $[\text{B}_{12}(\text{OH})_{12}]^{2-}$ dianions has been reported, and monoclinic $\text{Li}_2\text{B}_{12}\text{H}_{12}$ with similar crystal structure is also examined.

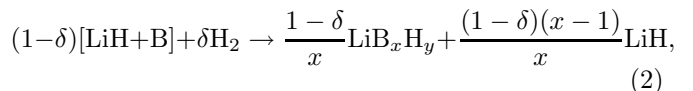
III. RESULTS AND DISCUSSIONS

A. Stability of candidate compounds : LiB_xH_y

Table I shows the calculated results on the structural parameters and the cohesive energies of LiB_3H_8 and $\text{Li}_2\text{B}_n\text{H}_n$ ($n = 5 - 12$). We denote the cubic $\text{Li}_2\text{B}_{12}\text{H}_{12}$ based on $\text{K}_2\text{B}_{12}\text{H}_{12}$ with type-1 and monoclinic $\text{Li}_2\text{B}_{12}\text{H}_{12}$ based on $\text{K}_2\text{B}_{12}(\text{OH})_{12}$ with type-2, respectively. Compared with the cohesive energy of two type of $\text{Li}_2\text{B}_{12}\text{H}_{12}$, the value of monoclinic $\text{Li}_2\text{B}_{12}\text{H}_{12}$ (type-2) is larger than that of type-1. Therefore, the type-2 $\text{Li}_2\text{B}_{12}\text{H}_{12}$ is easy to form. After the next paragraph, the only result concerning monoclinic $\text{Li}_2\text{B}_{12}\text{H}_{12}$ (type-2) is shown.

The enthalpy of formation for hydriding reactions including LiBH_4 from LiH (NaCl-type), α -B (rhombohedral), and H_2 molecule are given in Table II, where the zero-point energy corrections are not taken into consideration. They are provided using calculated cohesive energies of 2.3609 eV/atom for LiH , 6.2013 eV/atom for α -B, 2.2689 eV/atom for H_2 molecule, and 3.1501 eV/atom for LiBH_4 (orthorhombic $Pnma$ symmetry), respectively. The enthalpies of formation for $\text{Li}_2\text{B}_n\text{H}_n$ ($n = 10, 11, 12$) are more negative than that for LiBH_4 . Therefore these compounds have a great potential for generating in hydriding reactions from LiH and α -B as the intermediate phase of LiBH_4 .

In order to understand the stability of each compound intuitively, we represent the enthalpy of formation corresponding to the following reaction with hydrogen of δ mole in Fig. 1 :



where $\delta = (y-1)/(2x+y-1)$ shows the mole fraction of H_2 and $x \geq 1$. From Fig. 1, monoclinic $\text{Li}_2\text{B}_{12}\text{H}_{12}$ is formed as the intermediate compound of the hydriding/dehydriding reaction of LiBH_4 , because the actual reaction goes along the lowest state of enthalpy. Therefore, following hydriding/dehydriding process is proposed

TABLE I: Structural parameters and cohesive energies (E_{coh}) of the candidate compounds : LiB_xH_y . It is denoted that the cubic $\text{Li}_2\text{B}_{12}\text{H}_{12}$ based on $\text{K}_2\text{B}_{12}\text{H}_{12}$ with type-1 and monoclinic $\text{Li}_2\text{B}_{12}\text{H}_{12}$ based on $\text{K}_2\text{B}_{12}(\text{OH})_{12}$ with type-2, respectively.

Compound	Space group	Unit cell parameters	Atom		Atomic position			E_{coh} (eV/atom)
			Atom	Site	x/a	y/b	z/c	
LiB_3H_8	$Ama2$ (No.40)	$a = 9.188 \text{ \AA}$ $b = 8.813 \text{ \AA}$ $c = 5.763 \text{ \AA}$	Li	4b	0.0595	0.6321	0.25	3.3770
			B1	4b	0.1372	0.1335	0.25	
			B2	8c	0.3090	0.1331	0.0945	
			H1	4b	0.0690	0.2507	0.25	
			H2	4b	0.0684	0.1666	0.25	
			H3	8c	0.1386	0.5149	0.5190	
			H4	8c	0.1823	0.1333	0.0063	
			H5	8c	0.3619	0.2508	0.0186	
			$\text{Li}_2\text{B}_5\text{H}_5$	$R3m$ (No.160) (hexagonal axes)	$a = 5.599 \text{ \AA}$ $c = 16.763 \text{ \AA}$	Li1	3a	
Li2	3a	0				0	0.7513	
B1	3a	0				0	0.0876	
B2	3a	0				0	0.9295	
B3	9b	0.1070				0.8930	0.0084	
H1	3a	0				0	0.1595	
H2	3a	0				0	0.8586	
H3	9b	0.2270				0.7730	-0.0078	
$\text{Li}_2\text{B}_6\text{H}_6$	$Fm\bar{3}m$ (No.225)	$a = 7.968 \text{ \AA}$				Li	8c	0.25
			B	24e	0.1553	0	0	
			H	24e	0.3054	0	0	
$\text{Li}_2\text{B}_7\text{H}_7$	$I2$ (No.5)	$a = 5.691 \text{ \AA}$ $b = 9.836 \text{ \AA}$ $c = 5.625 \text{ \AA}$ $\beta = 77.39^\circ$	Li1	2b	0	0.1501	0.5	4.0850
			Li2	2b	0.5	0.2317	0	
			B1	2a	0	0.1564	0	
			B2	4c	-0.1871	0.0529	-0.1063	
			B3	4c	0.1160	-0.1087	0.0659	
			B4	4c	-0.1335	0.0087	0.1903	
			H1	2a	0	0.2792	0	
			H2	4c	-0.3463	0.0805	-0.2099	
			H3	4c	0.2215	-0.2030	0.1343	
$\text{Li}_2\text{B}_8\text{H}_8$	$I42m$ (No.121)	$a = 5.572 \text{ \AA}$ $c = 10.687 \text{ \AA}$	Li	4d	0	0.5	0.25	4.0920
			B1	8i	0.1032	0.1032	-0.1242	
			B2	8i	0.1631	0.1631	0.0304	
			H1	8i	0.2031	0.2031	-0.2112	
			H2	8i	0.3114	0.3114	0.0580	
$\text{Li}_2\text{B}_9\text{H}_9$	$R3$ (No.146) (hexagonal axes)	$a = 7.044 \text{ \AA}$ $c = 15.062 \text{ \AA}$	Li1	3a	0	0	0.2482	4.1326
			Li2	3a	0	0	0.8070	
			B1	9b	0.8087	0.9031	0.9508	
			B2	9b	0.8118	0.9047	0.0694	
			B3	9b	0.8661	0.7287	0.0096	
			H1	9b	0.6730	0.8346	0.8923	
			H2	9b	0.6756	0.8357	0.1281	
			H3	9b	0.7699	0.5322	0.0141	
$\text{Li}_2\text{B}_{10}\text{H}_{10}$	$I422$ (No.97)	$a = 6.196 \text{ \AA}$ $c = 10.356 \text{ \AA}$	Li	4d	0	0.5	0.25	4.2360
			B1	4e	0	0	0.1827	
			B2	16k	0.1942	-0.0809	0.0739	
			H1	4e	0	0	0.2984	
			H2	16k	0.3647	-0.1582	0.1070	
$\text{Li}_2\text{B}_{11}\text{H}_{11}$	$I2$ (No.5)	$a = 7.083 \text{ \AA}$ $b = 11.028 \text{ \AA}$ $c = 7.080 \text{ \AA}$ $\beta = 70.52^\circ$	Li1	2b	0	-0.1091	0.5	4.2397
			Li2	2b	0.5	-0.1083	0	
			B1	2a	0	-0.1264	0	
			B2	4c	0.1117	0.1190	-0.1120	
			B3	4c	0.0835	-0.0162	-0.2427	
			B4	4c	0.2425	-0.0162	-0.0840	
			B5	4c	0.1293	0.0825	0.1290	
			B6	4c	0.1448	-0.0795	0.1446	
			H1	2a	0	-0.2355	0	
			H2	4c	0.2016	0.2052	-0.2020	
			H3	4c	0.4160	-0.0284	-0.1910	
			H4	4c	0.1902	-0.0283	-0.4165	
			H5	4c	0.2133	0.1471	0.2127	
			H6	4c	0.2305	-0.1441	0.2300	
			$\text{Li}_2\text{B}_{12}\text{H}_{12}$ (type-1)	$Fm\bar{3}$ (No.202)	$a = 10.083 \text{ \AA}$	Li	8c	
B	48h	0				0.1448	0.0881	
H	48h	0				0.2490	0.1469	
$\text{Li}_2\text{B}_{12}\text{H}_{12}$ (type-2)	$P2_1/n$ (No.14)	$a = 7.358 \text{ \AA}$ $b = 9.556 \text{ \AA}$ $c = 6.768 \text{ \AA}$ $\beta = 92.26^\circ$	Li	4e	0.6747	0.6250	0.5323	4.3461
			B1	4e	0.6770	0.5392	0.1632	
			B2	4e	0.4447	0.5629	0.2239	
			B3	4e	0.5425	0.6760	0.0442	
			B4	4e	0.6915	0.5689	0.9022	
			B5	4e	0.6856	0.3922	0.9959	
			B6	4e	0.5329	0.3887	0.1933	
			H1	4e	0.8033	0.5642	0.2786	
			H2	4e	0.4008	0.6050	0.3840	
			H3	4e	0.5707	0.7983	0.0742	
			H4	4e	0.8252	0.6151	0.8271	
			H5	4e	0.8231	0.3231	0.9941	
H6	4e	0.5558	0.3097	0.3310				

TABLE II: The enthalpies of formation for the hydriding reaction of various compounds LiB_xH_y including LiBH_4 from LiH , $\alpha\text{-B}$, and H_2 molecule, where the zero-point energy corrections are not taken into consideration.

Hydriding reaction	Enthalpy of formation (kJ/mol H_2)
$\text{LiH} + 3\text{B} + 7/2\text{H}_2 \rightarrow \text{LiB}_3\text{H}_8$	-36
$2\text{LiH} + 5\text{B} + 3/2\text{H}_2 \rightarrow \text{Li}_2\text{B}_5\text{H}_5$	113
$2\text{LiH} + 6\text{B} + 2\text{H}_2 \rightarrow \text{Li}_2\text{B}_6\text{H}_6$	-42
$2\text{LiH} + 7\text{B} + 5/2\text{H}_2 \rightarrow \text{Li}_2\text{B}_7\text{H}_7$	-45
$2\text{LiH} + 8\text{B} + 3\text{H}_2 \rightarrow \text{Li}_2\text{B}_8\text{H}_8$	-32
$2\text{LiH} + 9\text{B} + 7/2\text{H}_2 \rightarrow \text{Li}_2\text{B}_9\text{H}_9$	-42
$2\text{LiH} + 10\text{B} + 4\text{H}_2 \rightarrow \text{Li}_2\text{B}_{10}\text{H}_{10}$	-87
$2\text{LiH} + 11\text{B} + 9/2\text{H}_2 \rightarrow \text{Li}_2\text{B}_{11}\text{H}_{11}$	-79
$2\text{LiH} + 12\text{B} + 5\text{H}_2 \rightarrow \text{Li}_2\text{B}_{12}\text{H}_{12}$	-125
$\text{LiH} + \text{B} + 3/2\text{H}_2 \rightarrow \text{LiBH}_4$	-75

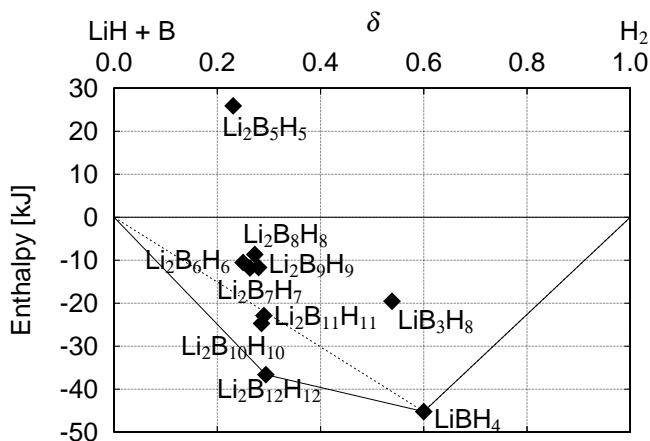
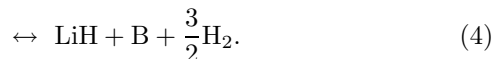
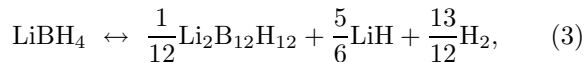


FIG. 1: Enthalpy of formation relative to $(1 - \delta)[\text{LiH} + \text{B}]$ and molecular H_2 of δ mole (reaction Eq.(2) in text), as a function of the mole fraction of H_2 , δ .

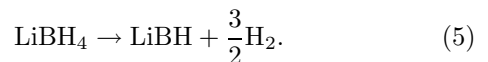
:



The enthalpy without zero-point energy effects and hydrogen content of the first reaction (Eq.(3)) are 56 kJ/mol H_2 and 10 mass% and those of the second reaction (Eq.(4)) are 125 kJ/mol H_2 and 4 mass%, respectively. These results agree with the experimental ones, which reported that 9 mass% of hydrogen are liberated in the hydrogen desorption peak in thermal desorption spectra of LiBH_4 mixed with SiO_2 -powder in Ref. 1. The enthalpy value of 56 kJ/mol H_2 for the first reaction is lower than computational one of 75 kJ/mol H_2 for direct dehydriding reaction of LiBH_4 (Eq.(1)).² So the hydrogen desorption and absorption can occur at low temperature and pressure comparatively by using this intermediate compound.

We also calculated other possible crystal structures such as $\text{Cu}_2\text{B}_{10}\text{H}_{10}$ -type²² and $[\text{Li}(\text{thp})_3]_2[\text{B}_{11}\text{H}_{11}]$ -type.²³ Moreover, we performed the calculation for the Γ -phonon frequencies of the candidate materials. If there was a soft-mode, we lowered crystal structure symmetry with moving the atoms along the direction of the soft-mode eigenvectors. The maximum gain of cohesive energy was 0.03 eV/atom for $\text{Li}_2\text{B}_6\text{H}_6$, however, no compound or crystal structure more stable than monoclinic $\text{Li}_2\text{B}_{12}\text{H}_{12}$ was found. The present calculation result on the energy of monoclinic $\text{Li}_2\text{B}_{12}\text{H}_{12}$ provides the upper limit value for the thermodynamic stability. In conclusion, the existence of the intermediate compound of LiBH_4 was predicted theoretically.

Recently Kang *et al.*²⁴ have reported that LiBH and LiB are the intermediate phases of LiBH_4 , and propose the dehydriding reaction of LiBH_4 through LiBH as follows :



We also performed the first-principles calculation of the orthorhombic phase of $Pnma$ LiBH . The reaction enthalpy for Eq.(5) is 1.30eV per LiBH_4 formula unit (84kJ/mol H_2), which is in good agreement with reported value of 1.28eV per LiBH_4 formula unit in Ref.24. On the other hand, the reaction enthalpy of Eq.(3) is 0.63eV per LiBH_4 formula unit. Therefore, the dehydriding reaction via the intermediate compound $\text{Li}_2\text{B}_{12}\text{H}_{12}$ is energetically more preferable one.

B. Intermediate compound : $\text{Li}_2\text{B}_{12}\text{H}_{12}$

Here we describe the fundamental properties, such as the crystal structure, the electronic structure, and the Γ phonon frequencies, on $\text{Li}_2\text{B}_{12}\text{H}_{12}$ which is expected as intermediate compound of LiBH_4 .

Optimized crystal structure model of monoclinic $\text{Li}_2\text{B}_{12}\text{H}_{12}$ is shown in Fig. 2. The bond lengths between B and H atom of $\text{Li}_2\text{B}_{12}\text{H}_{12}$ are 1.20 – 1.21 Å, and they are very close to those for LiBH_4 (1.23 – 1.24 Å) reported in Ref. 2. As for the B-B bond lengths of intra-icosahedron, the values of 1.779 – 1.811 Å for $\text{Li}_2\text{B}_{12}\text{H}_{12}$ are comparable to the experimental ones for the α -rhombohedral boron ($\alpha\text{-B}$) of 1.751 – 1.806 Å,²⁵ too. Since boron crystal has the icosahedral B_{12} cluster as a common structural component, the decomposition of $[\text{B}_{12}\text{H}_{12}]^{2-}$ anion into B_{12} cluster and hydrogen molecule is easy to understand.

Figure 3 shows the total and partial density of states (DOS) for $\text{Li}_2\text{B}_{12}\text{H}_{12}$, which denotes that it has the energy gap of 5.60 eV. Since there is little contribution of Li orbital for occupied states, $\text{Li}_2\text{B}_{12}\text{H}_{12}$ consists of Li^+ and $[\text{B}_{12}\text{H}_{12}]^{2-}$ ions. The orbitals of B and H hybridize each other and the feature of occupied states in DOS is analogous with the distribution of the computed energies of the bonding molecular orbitals in $[\text{B}_{12}\text{H}_{12}]^{2-}$.²⁶

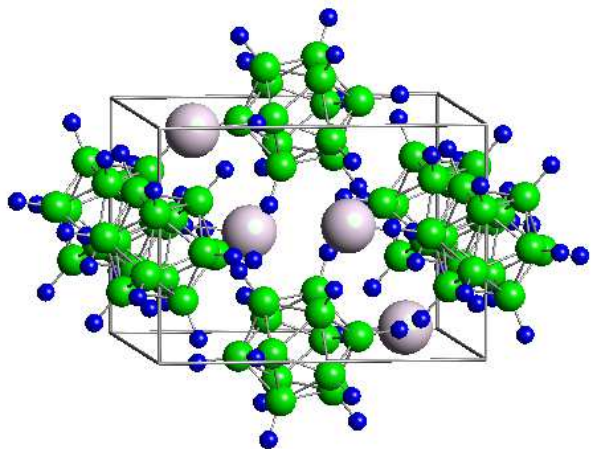


FIG. 2: (Color online) Crystal structure model of monoclinic $\text{Li}_2\text{B}_{12}\text{H}_{12}$ (type-2). Large, middle, and small spheres denote Li, B, and H atoms, respectively.

The Γ -phonon mode frequencies of monoclinic $\text{Li}_2\text{B}_{12}\text{H}_{12}$ have been calculated so that the vibrational properties can be compared with experiments easily and directly. The phonon density of states is shown in Fig. 4. It is divided into three regions in the same case as LiBH_4 . The first region is less than 300 cm^{-1} where the displacements of Li atoms are dominant. The second region is between 450 cm^{-1} and 1100 cm^{-1} where the B-H bond of $[\text{B}_{12}\text{H}_{12}]^{2-}$ dianions vibrates with changing in angle between them (bending modes), and the third region is between 2400 cm^{-1} and 2600 cm^{-1} where the interatomic distance of B-H bond is changing along bond axis (stretching modes). The frequencies of bending modes are lower than LiBH_4 described in Ref. 2, while stretching modes are higher.

The investigation using in situ Raman spectroscopy is effective for the confirmation of the short-range order or bonding of LiBH_4 .²⁷ We examine the atomistic vibrations of LiBH_4 during heating by in situ Raman spectroscopy, and the identification of spectra modes originating from $\text{Li}_2\text{B}_{12}\text{H}_{12}$ is now in progress.²⁸

C. Stability of complex anions : $[\text{B}_n\text{H}_n]^{2-}$

Finally, we consider the relation between the stability of the compounds $\text{Li}_2\text{B}_n\text{H}_n$ and those of complex anions $[\text{B}_n\text{H}_n]^{2-}$. The energies of the isolated $[\text{B}_n\text{H}_n]^{2-}$ are obtained using a face-centered-cubic supercell with $a = 20\text{ \AA}$. The single Γ point is used for the \mathbf{k} -point sampling. The energies for the charged systems are computed by adding uniform background charges and improved with Makov and Payne correction²⁹ for the interaction between periodic image charges.

Figure 5 shows the comparison of the formation energies, E_f^{solid} and E_f^{complex} , corresponding to the following

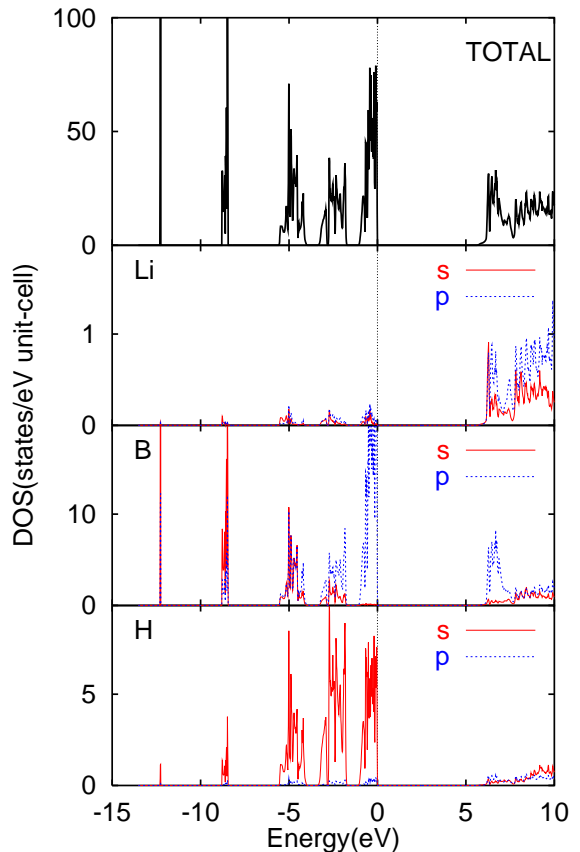


FIG. 3: (Color online) The total and partial densities of states (DOS) for $\text{Li}_2\text{B}_{12}\text{H}_{12}$. The energy is measured in eV relative to the top of valence states.

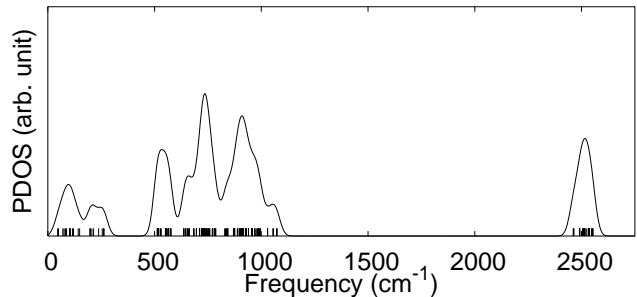
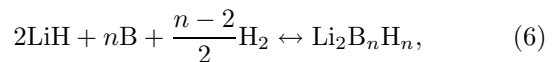
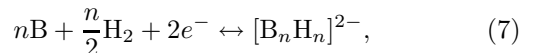


FIG. 4: Phonon density of states for monoclinic $\text{Li}_2\text{B}_{12}\text{H}_{12}$. The contribution of the TO Γ -phonon modes indicated by vertical bars is only taken into account and the Gaussian broadening with a width of 30 cm^{-1} is used.

reactions:



and



where the energies are normalized by the number of B-H pairs for comparison purposes. We can find a fairly good

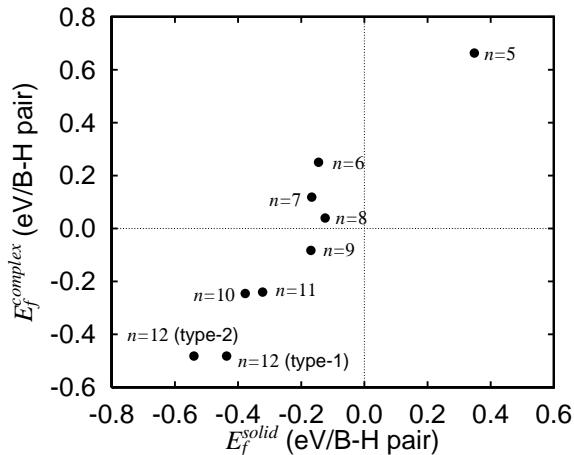


FIG. 5: Comparison of the formation energies, E_f^{solid} and $E_f^{complex}$, corresponding to the reactions Eq.(6) and Eq.(7) in text, respectively, where the energies are normalized by the number of B-H pairs.

correlation between both energies. This is probably due to the fact that the electrostatic interaction between Li^+ and $[\text{B}_n\text{H}_n]^{2-}$ is not sensitive to n and a large part of this energy cancels out with that of LiH in Eq. (6). Among the *closo*-type dianions considered here, $[\text{B}_{12}\text{H}_{12}]^{2-}$ is the most stable one.

LiBH_4 desorbs hydrogen at temperatures above the melting point. The latent heat of fusion has been reported³⁰ to be 0.078 eV/formula-unit for LiBH_4 and similar values are expected for $\text{Li}_2\text{B}_n\text{H}_n$, which is considerably smaller than the energy difference between $[\text{B}_{12}\text{H}_{12}]^{2-}$ and other *close*-type dianions. The stability of the $[\text{B}_{12}\text{H}_{12}]^{2-}$ anion supports our main conclusion in this study, that is, the intermediate phase suggested by the experiment is $\text{Li}_2\text{B}_{12}\text{H}_{12}$.

IV. SUMMARY

We have examined the stability of LiB_3H_8 and $\text{Li}_2\text{B}_n\text{H}_n$ ($n = 5 - 12$), which are the possible intermediate compounds of LiBH_4 , by the first-principles calculation. Our computational results for enthalpy of the hydriding reactions provide that monoclinic $\text{Li}_2\text{B}_{12}\text{H}_{12}$ is the most stable one among the candidates. The follow-

ing hydriding/dehydriding process of LiBH_4 is proposed: $\text{LiBH}_4 \leftrightarrow 1/12\text{Li}_2\text{B}_{12}\text{H}_{12} + 5/6\text{LiH} + 13/12\text{H}_2 \leftrightarrow \text{LiH} + \text{B} + 3/2\text{H}_2$. The hydrogen content of the first and the second reaction are 10 mass% and 4 mass%, respectively, which agree well with the thermal desorption spectra (TDS) experiment on LiBH_4 .¹ The heat of formation without zero point energy corrections for the first reaction, which is estimated from the solid state LiBH_4 with *Pnma* symmetry (not liquid LiBH_4), is 56 kJ/mol H_2 . This value is lower than that for the direct reaction ($\text{LiBH}_4 \leftrightarrow \text{LiH} + \text{B} + 3/2\text{H}_2$). Therefore, low temperature release of hydrogen can be expected by use of this intermediate compound.

We have calculated the electronic structure and the Γ -phonon frequencies of monoclinic $\text{Li}_2\text{B}_{12}\text{H}_{12}$. This compound has the energy gap of 5.60 eV and consists of Li^+ and $[\text{B}_{12}\text{H}_{12}]^{2-}$ ions. From the phonon density of states, it is predicted that its bending modes have lower frequencies than that of LiBH_4 ,² while stretching modes are higher. The identification of the experimental Raman spectra modes originating from $\text{Li}_2\text{B}_{12}\text{H}_{12}$ is now in progress.

The stability of *closo* borane complex anions $[\text{B}_n\text{H}_n]^{2-}$ was also examined. We found a fairly good correlation between the formation energies of the solid phases and the isolated dianions. This result supports the validity of the intermediate compound indicated in the TDS experiment being $\text{Li}_2\text{B}_{12}\text{H}_{12}$.

There are various kinds of borane, such as *nido*-type $[\text{B}_n\text{H}_{n+4}]$ and *arachno*-type $[\text{B}_n\text{H}_{n+6}]$, in addition to *closo*-type borane $[\text{B}_n\text{H}_{n+2}]$.³¹ The *nido* and *arachno* borane are derived from *closo* borane by removing one and two vertices, respectively. These generate the salts in the ionized state as well as *closo*-type dianions. These alkali metal salts are also the candidates of the intermediate compound of LiBH_4 . We will study the details of the hydriding/dehydriding process for LiBH_4 including the stability of these materials in future.

Acknowledgments

We wish to thank M. Matsumoto, R. Jinnouchi and S. Hyodo for helpful discussions. This work was partially supported by the New Energy and Industrial Technology Development Organization(NEDO), International Joint Research under the "Development for Safe Utilization and Infrastructure of Hydrogen" Project (2004-2005).

¹ A. Züttel, P. Wenger, S. Rentsch, P. Sudan, Ph. Mauron, and Ch. Emmenegger, J. Power Sources **118**, 1 (2003).

² K. Miwa, N. Ohba, S. Towata, Y. Nakamori, and S. Orimo, Phys. Rev. B **69**, 245120 (2004).

³ S. Orimo, Y. Nakamori, and A. Züttel, Mater. Sci. Eng. B **108**, 51 (2004).

⁴ P. Chen, Z. Xiong, J. Luo, J. Lin, and K. L. Tan, Nature

420,302 (2002).

⁵ Y. Nakamori and S. Orimo, Mater. Sci. Eng. B **108**, 48 (2004).

⁶ K. Miwa, N. Ohba, S. Towata, Y. Nakamori, and S. Orimo, Phys. Rev. B **71**, 195109 (2005).

⁷ D. Vanderbilt, Phys. Rev. B **41**, R7892 (1990); K. Laasonen, A. Pasquarello, R. Car, C. Lee, and D. Vanderbilt,

- ibid.* **47**, 10 142 (1993).
- ⁸ P. Hohenberg and W. Kohn, Phys. Rev. **136**, B864 (1964); W. Kohn and L. J. Sham, Phys. Rev. **140**, A1133 (1965).
- ⁹ J. P. Perdew, K. Burke, and M. Ernzerhof, Phys. Rev. Lett. **77**, 3865 (1996); **78**, 1396 (E) (1997).
- ¹⁰ D. R. Hamann, M. Schlüter, and C. Chiang, Phys. Rev. Lett. **43**, 1494 (1979) .
- ¹¹ A. M. Rappe, K. M. Rabe, E. Kaxiras, and J. D. Joannopoulos, Phys. Rev. B **41**, 1227 (1990) .
- ¹² S. G. Louie, S. Froyen, and M. L. Cohen, Phys. Rev. B **26**, 1738 (1982) .
- ¹³ A. Fukumoto and K. Miwa, Phys. Rev. B **55**, 11 155 (1997) .
- ¹⁴ V. Eyret, J. Comput. Phys. **124**, 271 (1996).
- ¹⁵ N. D. Mermin, Phys. Rev. **137**, A1441 (1965).
- ¹⁶ P. E. Blochl, O. Jepsen, and O. K. Andersen, Phys. Rev. B **49**, 16223 (1994).
- ¹⁷ K. Kunc and R. M. Martin, Phys. Rev. Lett. **48**, 406 (1982).
- ¹⁸ H. J. Deiseroth, O. Sommer, H. Binder, K. Wolfer, and B. Frei, Z. anorg. Allg. Chem. **571**, 21 (1989).
- ¹⁹ I.Y. Kuznetsov, D.M. Vinitskii, K.A. Solntsev, N.T. Kuznetsov, and L.A. Butman, Russian J. Inorg. Chem. **32**, 1803 (1987).
- ²⁰ I. Tiritiris and T. Schleid, Z. anorg. Allg. Chem. **629**, 1390 (2003).
- ²¹ T. Peymann, C. B. Knobler, S. I. Khan, and M. F. Hawthorne, J. Am. Chem. Soc. **123**, 2182 (2001).
- ²² R. D. Dobrott and W. N. Lipscomb, J. Chem. Phys. **37**, 1779 (1962).
- ²³ O. Volkov, W. Dirk, U. Englert, and P. Paetzold, Z. Anorg. Allg. Chem. **625**, 1193 (1999).
- ²⁴ J. K. Kang, S. Y. Kim, Y. S. Han, R. P. Muller, and W. A. Goddard III, Appl. Phys. Lett. **87**, 111904 (2005).
- ²⁵ B. Morosin, A. W. Mullendore, D. Emin, and G. A. Slack, in *Boron-Rich Solids*, edited by D. Emin, T. L. Aselage, C. L. Beckel, I. A. Howard, and C. Wood, AIP Conf. Proc. No. 140 (AIP, New York, 1986), p. 70.
- ²⁶ R. B. King, I. Silaghi-Dumitrescu, and A. Lupan, Inorg. Chem. **44**, 7819 (2005).
- ²⁷ S. Orimo, Y. Nakamori, G. Kitahara, K. Miwa, N. Ohba, S. Towata, and A. Züttel, J. Alloys Comp. **404-406**, 427 (2005).
- ²⁸ S. Orimo, Y. Nakamori, N. Ohba, K. Miwa, M. Aoki, S. Towata, and A. Züttel, Appl. Phys. Lett. , to be published.
- ²⁹ G. Makov and M. C. Payne, Phys. Rev. B **51**, 4014 (1995).
- ³⁰ M. B. Smith and G. E. Bass Jr., J. Chem. Eng. Data **8**, 342 (1963).
- ³¹ G. A. Olah, K. Wade, and R. E. Williams, *ELECTRON DEFICIENT BORON AND CARBON CLUSTERS*, (JOHN WILEY & SONS, 1991).